Vol. 733: 27–42, 2024
https://doi.org/10.3354/meps14560

MARINE ECOLOGY PROGRESS SERIES
Mar Ecol Prog Ser

Published April 4

Blue carbon biomass stocks but not sediment stocks or burial rates exhibit global patterns in re-established mangrove chronosequences: a meta-analysis

Daniel M. Alongi[1,*], Martin Zimmer[2,3]

[1]Tropical Coastal & Mangrove Consultants, Pakenham, Victoria 3810, Australia
[2]Leibniz Centre for Tropical Marine Research (ZMT) and University Bremen, 28359 Bremen, Germany
[3]IUCN SSC Mangrove Specialist Group, 1196 Gland, Switzerland

ABSTRACT: The re-establishment of mangrove forests is necessary to increase the quantity of sequestered carbon that would help to mitigate climate change. Determining long-term patterns of mangrove chronosequences is needed to develop a predictive capacity of carbon sequestration. We conducted a global meta-analysis of aboveground, belowground, sediment, and total ecosystem organic carbon (C_{ORG}) stocks and C_{ORG} burial rates (SCBR) in reforested, afforested, and naturally regenerated mangroves. Global patterns were detected for aboveground and belowground biomass C_{ORG} and ecosystem C_{ORG} stocks but not for sediment C_{ORG} stocks or SCBR. Mangrove trees increase carbon storage for up to a century, although they begin to plateau after 30–50 yr. Statistical analyses identified multiple variables as possible drivers and strong relationships between (1) mangrove biomass C_{ORG} stocks and forest age, (2) sediment and ecosystem C_{ORG} stocks, and (3) dominant mangrove species and environmental variables. Lack of a significant relationship between mangrove biomass and sediment blue carbon may be attributable to differences in environmental timescales and life histories between vegetation, sediment C_{ORG}, and subsurface sedimentary deposits. Sediment burial rates were nearly identical between those measured in re-established and natural forests, indicating that re-establishment of mangrove forests is a viable and predictable means of increasing long-term blue carbon sequestration. The global patterns suggest that predictive models can be constructed to improve forecasting of mangrove carbon sequestration, assisting in the sustainable development of mangrove plantations and mitigating climate change through market-based approaches.

KEY WORDS: Blue carbon · Global patterns · Chronosequence · Mangrove forest · Carbon stocks · Afforestation · Natural regeneration

1. INTRODUCTION

Mangrove forests, salt marshes, and seagrass meadows help regulate and mitigate anthropogenic greenhouse gas (GHG) emissions by sequestering organic carbon (C_{ORG}; known as 'blue carbon'), mostly in their sediments. These blue carbon ecosystems also provide a wide variety of essential ecosystem goods and services and play a key role in carbon biogeochemistry in the coastal ocean (Alongi 2018, Hilmi et al. 2021). Mangroves sequester more blue carbon than other coastal ecosystems, being the world's most C_{ORG}-rich habitat, and facilitate climate change mitigation (Alongi 2022). Despite a recent

*Corresponding author: dmalongi@outlook.com

reduction in deforestation (Friess et al. 2024), mangrove forests continue to be destroyed worldwide (Goldberg et al. 2020). To partly redress this imbalance, mangrove conservation and re-establishment (sensu Zimmer et al. 2022, henceforth including afforestation and natural regeneration) is necessary and feasible. Mangrove forests are also subjected to sea-level rise, erosion, and habitat loss due to extreme weather events. Such destruction and/or degradation leads to the exposure and oxygenation of sediment organic matter (SOM), resulting in microbial decay and the release of both CO_2 into the atmosphere (Lovelock et al. 2011) and porewater dissolved carbon via subsurface groundwater discharge (Alongi 2020a).

Mangroves are well suited for a market-based approach to conserve forests, including payments for ecosystem services (PES) and carbon finance marketing schemes, because of their ability to rapidly sequester large amounts of blue carbon, their high level of resistance and resilience to disturbance, and their extensive provision of other ecosystem services, such as providing coastal protection, habitat for species of importance for fisheries, and wood for fuel and housing. Such a socioeconomic approach may help to address the underlying drivers of mangrove loss and provide direct economic incentives for conservation, sustainable management, or re-establishment. Market-based strategies to maximize the net gain of blue carbon, therefore, must focus not only on enhancing forest production, including sustainable (non-destructive) use of wood resources, but also on facilitating the preservation and enhancement of C_{ORG} stocks and burial capacity in mangrove sediment and the accumulation of C_{ORG} in tree biomass as forests grow and mature. While much tree C_{ORG} is eventually lost due to clear-cutting or natural senescence and subsequent decay and exported to adjacent coastal waters, 75–95% of mangrove C_{ORG} is stored belowground (Alongi 2014) to depths of several meters, especially in dead roots and rhizomes and as recalcitrant organic matter (OM) of multiple autochthonous and allochthonous origins (including ancient C_{ORG} in deep sediments deposited prior to mangrove re-establishment originating from at least the early Holocene; Zimmer & Helfer 2021).

It is necessary to understand not only how C_{ORG} accumulates in restored mangrove environments, especially with increasing forest age, but it is highly desirable to understand the drivers of sequestration as well as OM decay and GHG emissions (Rosentreter et al. 2021, 2023), including the patterns of blue carbon dynamics and change over time. It is well established that blue carbon stocks increase in mangrove plantations in locations such as Southeast Asia, China, and India (Thant et al. 2012, Gevaña et al. 2017, Hien et al. 2018, Kathiresan et al. 2021, Wang et al. 2021), but to date, no attempts have been made to establish whether such patterns are global. Such information would be very useful to help realise and model such changes to increase the accuracy of predictions regarding which conditions are likely to promote the sequestering of blue carbon in re-established forests (Lovelock et al. 2022). The sustainable development of mangrove restoration is in its early stages, with many environmental, technical, societal, economic, and political problems and barriers, such that most attempts to re-establish mangroves for blue carbon have been unsuccessful (Friess et al. 2024). Resolving knowledge gaps can encourage re-establishment projects, as such improvements may increase success rates and support new methods in blue carbon accounting by reducing uncertainty, including measures of improved biodiversity and societal conditions.

To develop sustainable management frameworks and to understand the best and most efficient methods of mangrove re-establishment, blue carbon resources need to be fully integrated into climate change mitigation and conservation strategies on local, national, and global scales (Hilmi et al. 2021). This paper describes a meta-analysis of blue carbon changes in biomass and sediment in re-established (including afforested) mangrove plantations, using a chronosequence ('space for time') approach. Our objective was to develop a predictive capacity of such changes over time as a first effort in providing robust, empirical evidence for assisting in facilitating modelling that, if successful, could reduce costs and increase uptake of restoration projects via financial markets.

2. MATERIALS AND METHODS

2.1. Literature search and screening

A systematic literature search was conducted by following the PRISMA protocol (Page et al. 2021). The search was conducted with no restriction of publication year or type of publication (see Fig. A1 in the Appendix for PRISMA protocol), using the ISI Web of Science Core Collection, Google Scholar, China National Knowledge Infrastructure, Elsevier Scopus and Science Direct platforms, and the Sustainable Wetlands Adaptation and Mitigation Program

(SWAMP) data (https://www2.cifor.org/swamp) and various combinations of the following keywords: 'mangrove', 'carbon', 'organic carbon', 'blue carbon', 'carbon stocks', 'mangrove forest', 'mangrove swamp', 'mangrove wetland', 'ecosystem', 'aboveground', 'belowground', 'soil', 'sediment', 'forest age', 'chronosequence', 'biomass', 'restoration', 'replant', 'rehabilitation', 'regeneration', 'sequestration', 'burial', 'reforestation', 're-establishment', 'afforestation', 'natural', 'plantation', 'organic carbon', and 'organic matter'. Earlier references or data in peer-reviewed publications (Breithaupt et al. 2012, Alongi 2018, Su et al. 2021, Breithaupt & Steinmuller 2022, Song et al. 2023) were also taken into consideration. In total, 4568 articles were identified (in English, Bahasa Indonesia, and Mandarin), of which 4209 were excluded after an initial screening and a second screening of the title, abstract, and full text.

Of the remaining 359 articles, 121 were discarded after not meeting at least one of the following criteria: (1) contains sufficient detail to judge whether methodology and level of replication were appropriate and based on published studies; (2) quantitative data were only from empirical field studies with individual forest ages (not age intervals and not <3 mo) and mangrove species clearly stated; (3) sediment data on percent total organic carbon (%TOC) and C_{ORG} stocks were measured to a minimum depth of 50 cm and standardized if necessary to a maximum depth of 1 m; if <1 m depth, we assumed that the carbon density of the unmeasured deeper sediment to 1 m was the same as that of the deepest measured horizon, which slightly overestimated C_{ORG} stocks; (4) detailed data was provided on the methods used for active restoration, natural regeneration, and afforestation (where mangroves did not previously exist in that location); (5) carbon data was provided for at least one of the 4 mangrove carbon pools (aboveground biomass, belowground biomass, sediment organic carbon (SOC), or total ecosystem carbon) as well as sediment C_{ORG} burial rates (SCBR) (all carbon pools and rates are as defined by Howard et al. 2014); (6) a description of prior landuse, including abandoned aquaculture and/or agriculture sites built by removing existing mangroves, unsustainable harvesting due to timber use and forest losses due to defoliation and/or alteration of tidal flow as a result of construction; and (7) no disturbances interfered with or disrupted restoration during the study. In total, 238 articles were included in the meta-analysis, representing 580 individual restoration sites. The full list of articles considered in the meta-analysis is included in Table S1 in Supplement 1 at www.int-res.com/articles/suppl/m733p027_supp1.pdf. Data from sites where *Lagunculariaracemosa*, *Ceriops tagal*, *C. decandra*, and *Aegiceras corniculatum* were dominant species were not included in the meta-analysis due to very few observations (<10 at 5 locations).

Data were extracted from these articles, and for those containing only graphed data, we determined values from figures using the Get Data Graph Digitizer (https://getdata-graph-digitizer.software.informer.com). Mangrove forest biomass was obtained either from harvesting or allometry, with aboveground biomass being the sum of leaf, branch, and stem dry weight and prop roots when *Rhizophora* spp. were present. Belowground biomass was obtained from coring methods to measure living coarse and fine roots (dry weight) multiplied by the ratio of core area to sediment surface area. Stem diameter-at-breast-height and tree height were used to calculate above- and belowground biomass by allometric equations in Komiyama et al. (2008) with correction for root biomass in Adame et al. (2017). For some articles, above- and belowground biomass data were calculated if total biomass and shoot:root ratios were provided as C_{ORG} content; if not provided, these data were estimated from dry weight biomass and/or SOM using conversion factors in Fourqurean et al. (2015) and Breithaupt et al. (2023), with coefficients of variation of 5.2 and 5.7, respectively. If belowground root carbon (BGB-C) was not separated from SOC data, a conversion factor of BGB-C:SOC ratio of 14% was used (Alongi 2020b).

Additional data collected for each site were latitude, longitude, annual water temperature, porewater or tidal water salinity, annual average rainfall, and sediment % TOC, total nitrogen (% TN), and molar C:N ratio, when available. Mangrove necromass and pneumatophore biomass were excluded from the analysis due to few data and/or variable methodologies used. All data can be found in Excel files in Supplement 2 at www.int-res.com/articles/suppl/m733p027_supp2.xlsx.

Burial rates from the literature, starting with the data sets in Breithaupt et al. (2012), Alongi (2020a), and Breithaupt & Steinmuller (2022) and collated as specified in Breithaupt & Steinmuller (2022) were either stated explicitly or calculated via one of 2 equations in which SCBR (g C_{ORG} m^{-2} yr^{-1}) was calculated by (1) multiplying the accretion rate (cm yr^{-1}) by dry bulk density (g cm^{-3}) by % TOC or (2) multiplying mass accumulation rate (g m^{-2} yr^{-1}) by % TOC. Most published SCBR were derived from sediment cores that were dated using radiometric methods (^{210}Pb, ^{137}Cs), although some studies calculated rates

relative to event horizons from earthquakes or deforestation that occurred on known dates or over known time frames. Burial rates obtained via estimates rather than empirical measurements were excluded from our statistical analyses due to potentially large uncertainties.

2.2. Data analysis

All carbon–forest age relationships were explored using the best-fit global curve-fitting program in the Sigmaplot v.15.0.0.13 package (Systat Software). The Shapiro-Wilk test was used to determine whether each compiled data set met the assumptions of normality. If this assumption was violated, data were ln transformed; forest age was ln transformed for some relationships to obtain the best-fit equations. Two-way ANOVAs were performed with forest age and dominant species as factors without replication with all age and species data ln transformed prior to ANOVA to meet normality and homogeneity of variance assumptions. Post hoc species comparisons were made using Dunn's multiple comparisons test. A Kruskal-Wallis 1-way ANOVA on ranks test was performed to compare SCBR between re-established and natural forests, as data did not meet parametric assumptions after data transformation. Pearson product-moment correction analysis was conducted to examine relationships between environmental factors and blue carbon stocks. A significance value of $p < 0.05$ was accepted, except where noted.

Principal component analysis (PCA) was conducted to identify possible patterns among dependent variables: aboveground, belowground, and total ecosystem biomass C_{ORG}, sediment C_{ORG} stocks, SCBR, dominant species, forest age, latitude, sediment % TOC, salinity, rainfall, and temperature; sediment % TN and C:N ratios were excluded from the analysis due to the small sample size (<21% of total sites) as per the assumptions and criteria of PCA analysis (Syms 2019).

All raw data (including the latitude and longitude of all plantations) are presented in Excel files in Supplement 2.

3. RESULTS

3.1. Aboveground and belowground C_{ORG} biomass with forest age

Aboveground and belowground mangrove biomass C_{ORG} increased significantly with forest age (Figs. 1 & 2) with the best-fit equation being a 3-parameter, power function on ln-transformed aboveground biomass data. The best-fit regression for the belowground biomass was a 2-parameter power function performed on ln-transformed data.

There were no significant differences among species in aboveground biomass C_{ORG} (Fig. 3a) or in belowground biomass C_{ORG} (Fig. 3b) as indicated by a 2-way ANOVA (Table 1). However, there were significant differences in forest age (Table 1).

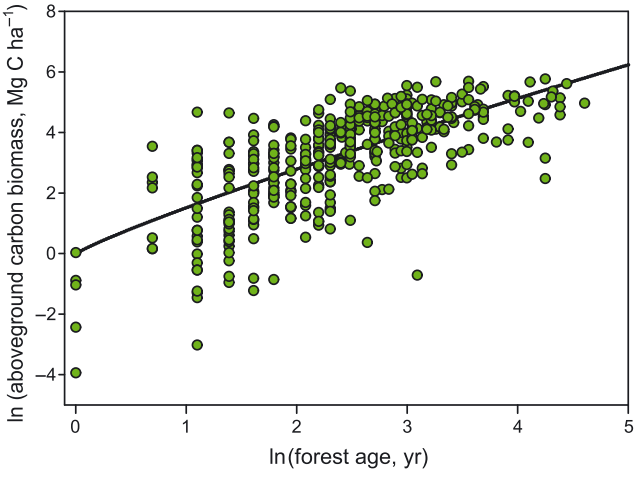

Fig. 1. Global pattern of aboveground organic carbon (C_{ORG}) biomass with increasing forest age. The best-fit power curve, $y = -1.76 + 3.0543(x^{0.5742})$, $r^2 = 0.5118$, $F_{3,433} = 1364.4$; $p < 0.0001$, was significant using ln-transformed aboveground C_{ORG} biomass and age data

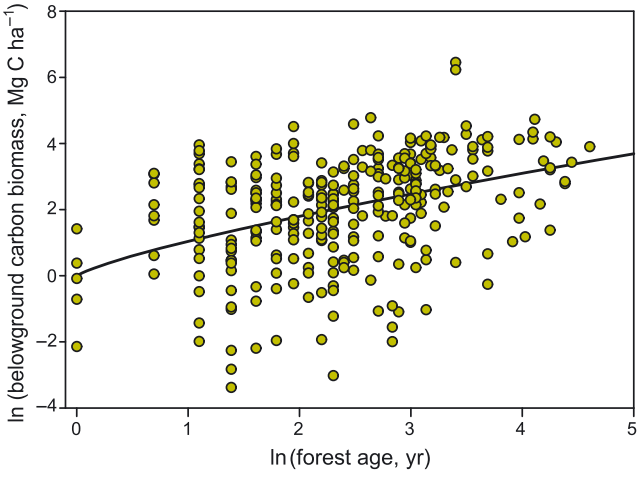

Fig. 2. Global pattern of belowground organic carbon C_{ORG} biomass with increasing forest age. The best-fit power curve, $y = 1.05666(x^{0.7791})$, $r^2 = 0.152$, $F_{2,304} = 311.2$; $p < 0.0001$, was significant using ln-transformed belowground C_{ORG} biomass and age data

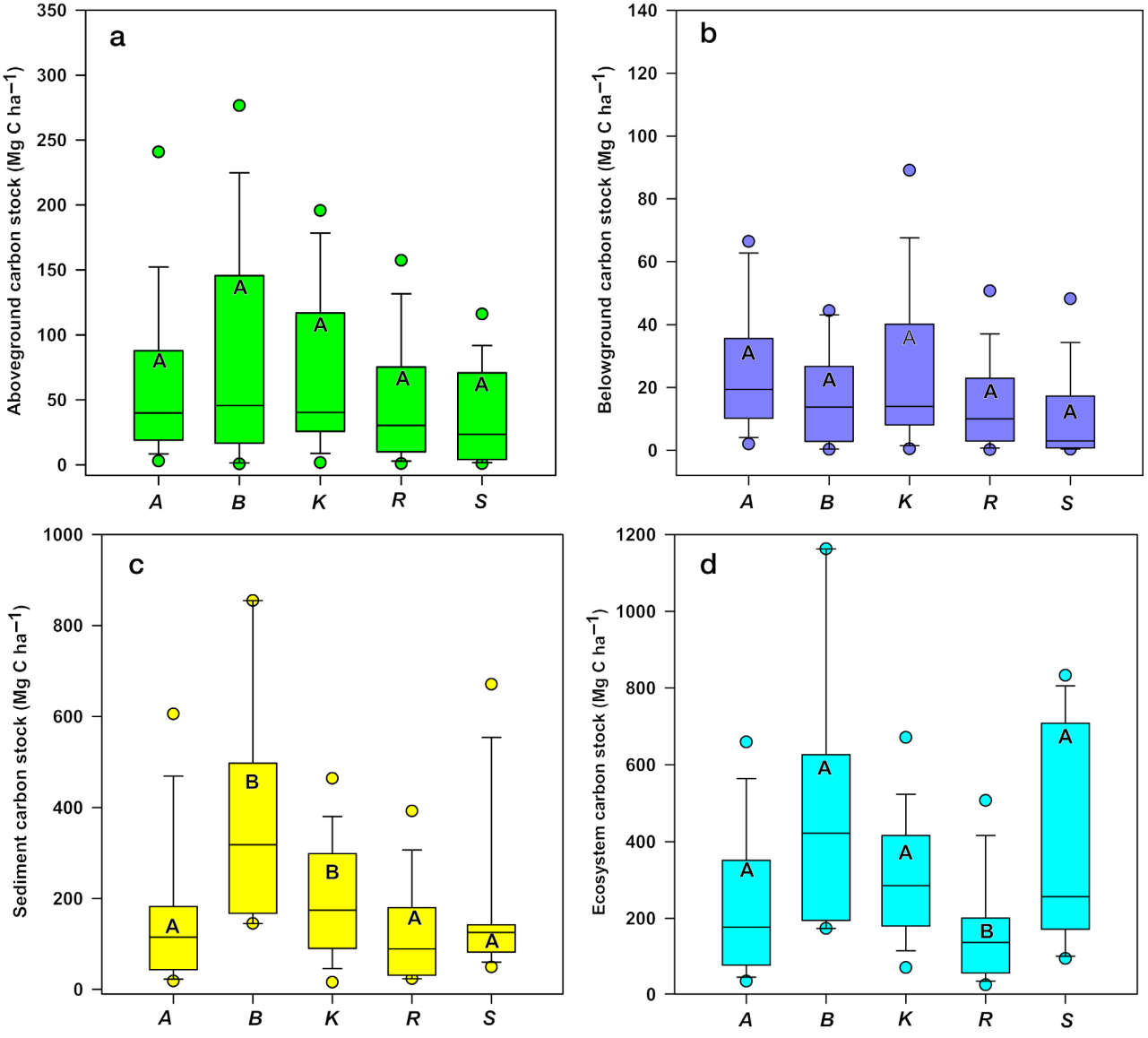

Fig. 3. Boxplots of species groups (*A: Avicennia marina*, *A. officinalis*, *A. germinans*, *A. alba*; *B: Bruguiera gymnnorhiza*, *B. cylindrica*; *K: Kandelia obovata*, *K. candel*; *R: Rhizophora apiculata*, *R. mucronata*, *R. stylosa*, *R. mangle*; *S: Sonneratia apetala*, *S. caseolaris*) with stand age in (a) aboveground organic carbon (C_{ORG}) biomass, (b) belowground C_{ORG} biomass, (c) sediment C_{ORG} stock, and (d) total ecosystem C_{ORG} stocks. Horizontal line in each box: mean; lower and upper hinges: 25th and 75th percentiles; error bars: 95% confidence intervals; points: outliers. Uppercase letters in common between means indicate no significant difference (e.g. A and A are statistically the same; A and B are statistically different)

Aboveground biomass C_{ORG} stocks correlated significantly but weakly and inversely with latitude ($r = -0.11$, $p < 0.01$) and salinity ($r = -0.15$, $p < 0.002$), and positively with sediment C_{ORG} ($r = 0.25$, $p < 0.0001$) and % TOC ($r = 0.29$, $p < 0.001$). Belowground biomass C_{ORG} stocks correlated significantly and positively only with latitude ($r = 0.13$, $p < 0.02$), sediment C_{ORG} ($r = 0.49$, $p < 0.001$), and % TOC ($r = 0.28$, $p < 0.001$).

3.2. Sediment C_{ORG} stock changes with forest age

The relationship between sediment C_{ORG} stocks and forest age (Fig. 4) was not significant (Table 1), but there were differences among species (Fig. 3c). Dunn's multiple comparisons tests indicated that sediment C_{ORG} stocks were greater in *Bruguiera gymnorrhiza*, *B. cylindrica* (mean ±1 SD = 370.4 ± 225.5) and *Kandelia obovata*, *K. candel* (205.1 ± 143.1) re-establishment sites than at sites dominated

Table 1. Significance of mangrove carbon biomass, sediment carbon, ecosystem carbon, and sediment C_{ORG} burial rates in relation to species and forest age (2-way ANOVA; *p < 0.05, **p < 0.01, ***p < 0.001). C_{ORG}: organic carbon

Component	*F*	df	p
Aboveground biomass C_{ORG} stock			
Species	1.18	4,444	0.322^{ns}
Forest age	5.79	73,444	<0.001***
Belowground biomass C_{ORG} stock			
Species	0.79	4,292	0.541^{ns}
Forest age	6.52	54,292	<0.001***
Sediment C_{ORG} stock			
Species	2.69	4,342	0.051^{ns}
Forest age	1.35	70,342	0.65^{ns}
Ecosystem C_{ORG} stock			
Species	3.62	4,244	<0.001***
Forest age	2.62	69,244	<0.001***
Sediment C_{ORG} burial rate			
Species	1.12	4,158	0.052^{ns}
Forest age	1.42	40,226	0.053^{ns}

by *Avicennia marina*, *A. officinalis*, *A. germinans*, *A. alba* (170.1 ± 192.1), *Rhizophora apiculata*, *R. mucronata*, *R. stylosa*, *R. mangle* (124.0 ± 106.1), and *Sonneratia apetala*, *S. caseolaris* (172.9 ± 172.5).

Sediment C_{ORG} stocks correlated positively with %TOC (r = 0.33, p < 0.001), temperature (r = 0.25, p < 0.001), and annual rainfall (r = 0.29, p < 0.001). Sediment C_{ORG} stocks correlated negatively with latitude (r = −0.41, p < 0.001). Sediment % TOC correlated positively with forest age (r = 0.16, p < 0.01), temperature (r = 0.25, p < 0.001), annual rainfall (r = 0.26, p < 0.001), and salinity (r = 0.14, p < 0.05). Sediment % TN averaged 0.19 ± 0.02%, with a median of 0.12% and a range of 0.013–1.42%. Sediment molar C:N ratio averaged 19 ± 1, with a median of 14.5 and a range of 6.5–76.8.

3.3. Ecosystem C_{ORG} stock trajectories with forest age

Ecosystem C_{ORG} stocks increased significantly (Fig. 5) with forest age, with linear regression being the best-fit model (Table 1). A 2-way ANOVA indicated significant forest age and species differences (Table 1). Dunn's multiple comparisons tests showed that ecosystem C_{ORG} stocks (Fig. 3d) of *Rhizophora* spp. (173 ± 147) were significantly less than those of the other species (Fig. 3d). Sediment C_{ORG} stocks accounted for an average of 67% and aboveground and belowground C_{ORG} stocks accounted for 26 and 7%, respectively, of total ecosystem C_{ORG} stocks.

Ecosystem C_{ORG} stocks correlated inversely with latitude (r = −0.22, p < 0.001) and sediment % TN (r = −0.26, p < 0.05) and positively with temperature (r = 0.16, p < 0.01), annual rainfall (r = 0.18, p < 0.001), % TOC (r = 0.50, p < 0.0001), sediment C_{ORG} (r = 0.93, p < 0.0001), aboveground biomass C_{ORG} (r = 0.52, p < 0.0001), and belowground biomass C_{ORG} (r = 0.68, p < 0.0001).

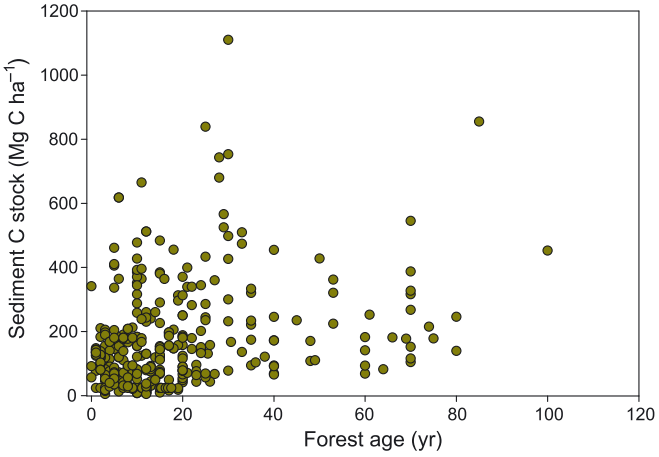

Fig. 4. Plot of global sediment organic carbon (C_{ORG}) stocks in restored, afforested, and naturally regenerated forests with increasing age. The relationship (using either transformed or untransformed data) was not significant (p > 0.05). Sediment C_{ORG} stocks were significant among some species (see Fig. 3c)

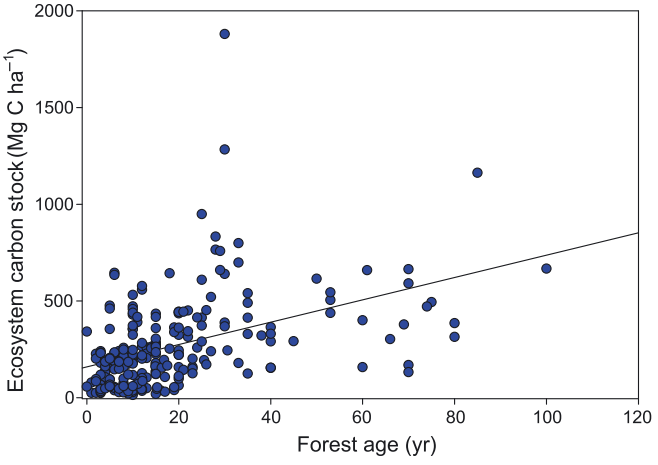

Fig. 5. Global pattern of total ecosystem organic carbon (C_{ORG}) stocks with increasing forest age. Best-fit linear regression on untransformed data, $y = 159.343 + 5781x$, $r^2 = 0.201$, $F_{1,226} = 56.559$; p < 0.001. Total ecosystem C_{ORG} stocks of *Rhizophora* species were significantly less than the other species (see Fig. 3d)

3.4. Sediment C_{ORG} burial rates

The relationship between sediment C_{ORG} burial rates and forest age (Fig. 6) was not significant

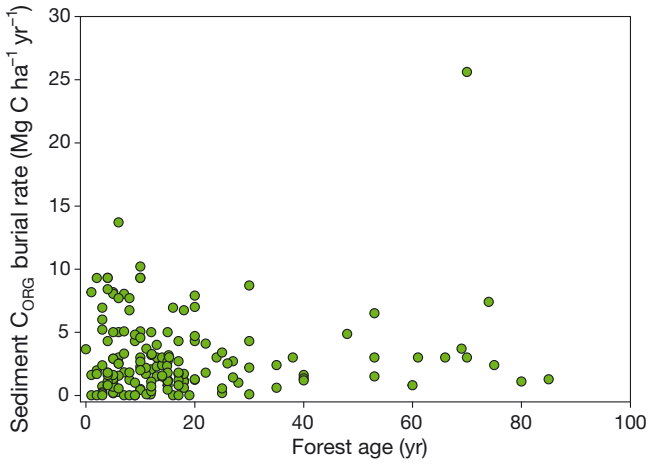

Fig. 6. Global sediment organic carbon (C_{ORG}) burial rates in restored, afforested, and naturally regenerated forests with increasing age. The relationship (using either transformed or untransformed data) was not significant ($p > 0.05$)

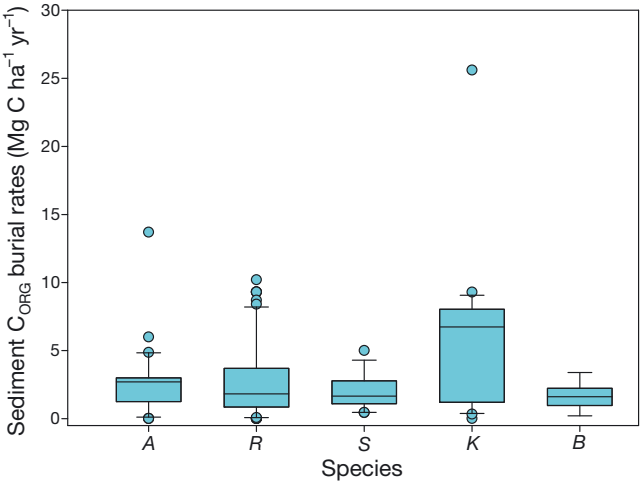

Fig. 7. Boxplots of species groups (*A*: *Avicennia marina*, *A. officinalis*, *A. germinans*, *A. alba*; *R*: *Rhizophora apiculata*, *R. mucronata*, *R. stylosa*, *R. mangle*; *S*: *Sonneratia apetala*, *S. caseolaris*; *K*: *Kandelia obovata*, *K. candel*; *B*: *Bruguiera gymnnorhiza*, *B. cylindrica*) with stand age, indicating no significant differences in sediment organic carbon (C_{ORG}) burial rates among the 5 groups. Boxplot parameters as in Fig. 3

(Table 1), nor were there significant differences among species (Fig. 7). Burial rates correlated only inversely with salinity (Pearson product moment, $r = -0.30$, $p = 0.0017$) and sediment C:N ratio ($r = 0.35$, $p = 0.0183$). C_{ORG} burial rates in sediments of re-established mangrove stands ranged from 0.7 to 2560 g C m^{-2} yr^{-1}, averaging 283 ± 326 g C m^{-2} yr^{-1}, with a median of 182 g C m^{-2} yr^{-1}. SCBR in natural terrigenous mangrove forests (excluding carbonate settings) ranged from 2.3 to 1749 g C m^{-2} yr^{-1}, averaging 226 ± 247 g C m^{-2} yr^{-1}, with a median of 154 g C m^{-2} yr^{-1}. The differences between re-established and natural SCBRs were not significantly different (Kruskal-Wallis 1-way ANOVA on ranks, $p > 0.05$).

3.5. PCA

The PCA (Fig. 8) resulted in a significant difference in the eigenvalues ($\chi^2 = 3332$ df = 45.00, $p < 0.001$), with eigenvalues PC1, PC2, and PC3 explaining 33.50, 22.46, and 12.93% of the cumulative variation of 68.89%, respectively. Component loadings for variables within the PC1 and PC2 dimensional space aggregated into 3 groups (Fig. 8). One group consisted of 'forest age' and above- and belowground biomass C_{ORG} (AGB-C, BGB-C) with the second grouping comprising % TOC and sediment and ecosystem C_{ORG} stocks (SOC, Ecosystem-C). The third cluster was formed by environmental factors (salinity, rainfall, temperature) and dominant species (species).

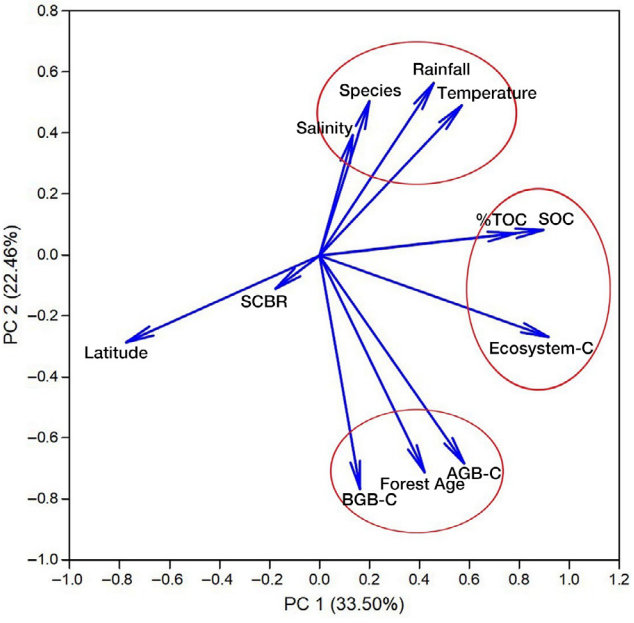

Fig. 8. Principle component analysis (PCA) in a 2-dimensional plot of eigenvalues (PC1) and PC2. Percentage values in parentheses on the axis labels indicate the variation of each eigenvalue. Red ellipses identify 3 groups with a high level of similarity in the PCA matrix. One ellipse encompasses species with environmental variables (salinity, rainfall, temperature); the middle ellipse encompasses percent sediment total organic carbon stocks (% TOC), sediment organic carbon (SOC) stocks and total ecosystem organic carbon (C_{ORG}) stocks (Ecosystem C); and the third ellipse encompasses forest age (Forest Age) and aboveground C_{ORG} (AGB-C) and belowground C_{ORG} (BGB-C) biomass. Both sediment carbon burial rates (SCBR) and latitude with negative PC1 and PC2 scores are not closely linked to the other variables

The factors latitude and SCBR were not associated with any variables. These groupings were supported by the high scores within the correlation matrix.

4. DISCUSSION

4.1. Global patterns in mangrove biomass C_{ORG}

The significant global patterns of mangrove aboveground and belowground C_{ORG} with increasing stand age followed growth curves like those found for individual plantations (Table 2), with considerable variability with age, species, and regions, and a decrease in the rate of growth, to approach an equilibrium during the latter stages of forest development. This variability likely reflects species differences and differences in stand history and regions, and the lack of a strong sediment C_{ORG}–forest age relationship. Both Lovelock et al. (2022) for aboveground biomass carbon and Song et al. (2023) for afforested versus restored plantation biomass carbon measured significant exponential growth curves with significant variations with forest age. Regional variations in mangrove aboveground biomass C_{ORG} over chronosequences of development showed wide differences among countries with varying climates and other environmental factors (Lovelock et al. 2022). The data further indicate that different levels of mature standing biomass were achieved between 20 and 40 yr of age. Our growth curves suggest a slight decline in growth rate, but an overall increase in C_{ORG} storage until at least 80–100 yr. These variations partly explain the significant, but weak, correlations between mangrove biomass C and stand age (Fig. 3a,b). Our biomass carbon–age curves are somewhat different than those of Song et al. (2023) for several reasons, as our analyses include (1) naturally regenerated forests, (2) stands older than 40 yr, and (3) more data points for above- and belowground biomass C_{ORG} (558 data points in Song et al. 2023 vs. 970 points in our analyses).

These positive relationships were weak, but this is unsurprising considering that multiple species and locations encompass and mask variations in regional growth patterns and environmental history, affecting both plant growth and development. In some regions, C_{ORG} storage capacity differs among species (Kathiresan et al. 2013, He et al. 2020, Chen et al. 2023) as is the case of greater C_{ORG} stores in total plant biomass of *Kandelia obovata* versus adjacent *Sonneratia apetala* plantations in China (He et al. 2020). Earlier work (Kathiresan et al. 2013) found that *Avicennia marina* displayed 75% greater C_{ORG} burial than *Rhizophora mucronata* in 1–17.5 yr old stands; more recently, Chen et al. (2023) found that *A. marina* had greater C_{ORG} ecosystem stocks than *K. obovata* stands, but only at elevations below mean sea level.

Mangrove growth is strongly linked to many drivers that vary by species and location, including sediment fertility, temperature, salinity, extent of tidal inundation, and anoxia (Alongi 2009). Biomass C_{ORG} did not correlate strongly with edaphic drivers, such as % TN or sediment C:N ratio, likely reflecting the fact that multiple factors play a role in regulating forest growth. Both above- and belowground biomass C_{ORG} correlated strongly with sediment C_{ORG} stocks and % TOC, likely reflecting OM enrichment with forest maturity.

At the stand scale, species richness and functional diversity of the mangrove trees, including their functional distinctiveness, mediate C_{ORG} stocks in above- and belowground biomass (Rahman et al. 2021). In at least one case of naturally regenerated forests (Yu et al. 2021), the contribution of biomass C_{ORG} stock to total ecosystem C_{ORG} stock increased with age, while the sediment showed the opposite pattern; the annual accumulation rate of ecosystem C_{ORG} stocks decreased along an age gradient of 15, 45, and 80 yr. Thus, while most biomass C_{ORG} patterns are positive with time, not all are (Table 2). Our PCA points to a strong mangrove biomass C_{ORG}–age relationship with negative scores in the 2-dimensional PC space (Fig. 8).

Reforested stands have greater blue carbon storage potential per hectare than afforested stands, and this finding has been attributed to favourable positioning in the intertidal zone, high nitrogen availability, and lower salinity (Song et al. 2023). Naturally regenerated stands were not included in their analysis, but data from individual stands indicate similar growth curves in comparison with reforested and afforested plantations for the same age. For instance, carbon burial in naturally regenerated stands consisting of *Ceriops decandra*, *Bruguiera sexangulata*, and *Aegiceras corniculatum* was greater than in restored plantations measured in the Ayeyarwady delta, Myanmar (Thant et al. 2012), where aboveground and belowground biomass C_{ORG} was greater than in plantations of *A. marina*, *A. officinalis*, and *S. apetala.*

Despite variations, mangrove ecosystems can store increasing amounts of blue carbon for at least 40–60 yr (Lovelock et al. 2022), a trend reminiscent of carbon storage in tropical secondary lowland forests, where C_{ORG} accumulates rapidly during early stages but plateaus as forests attain maturity (Sierra et al.

Table 2. Selected studies of mangrove chronosequence trajectories (Chrono.) of aboveground (AGBC) and belowground (BGBC) carbon biomass, sediment carbon stocks (SOC), sediment carbon burial rates (SCBR), and ecosystem carbon stocks (ECS). Trajectory abbreviations: (—) not available; L+: linear increase; E+: exponential or power increase; Q+: quadratic increase; 0: no trajectory. REM: re-establishment method: R: restoration; A: afforestation; NR: natural regeneration

Location	REM	Dominant species	Chrono. (yr)	Trajectory					Reference
				AGBC	BGBC	SOC	SCBR	ECS	
Qi'ao Island, China	R	*Sonneratia apetala*	1—40	L+	L+	L+	—	L+	Yu et al. (2020)
Qi'ao Island, China	R	*S. apetala*, *Kandelia obovata*	11—60	L+	L+	0	0	L+	Zhang et al. (2022)
NSW, Australia	NR	*Avicennia marina*	5—80	E+	—	—	—	—	Lovelock et al. (2022)
SA, Australia	NR	*A. marina*	5—90	E+	—	—	—	—	Lovelock et al. (2022)
Pichavarum, India	R	*Rhizophora mucronata*	1—17.5	L+	—	—	—	—	Kathiresan et al. (2013)
Pichavarum, India	R	*A. marina*	12—21	L+	L+	0	0	L+	Kathiresan et al. (2021)
Len R., Vietnam	R	*K. obovata*, *S. caseolaris*	2—27	E+	E+	L+		E+	Hieu et al. (2017)
Moloka'i Island, Hawaii	NR	*R. mangle*	69—75	E+	E+	0	0	E+	Soper et al. (2019)
Lingayen Gulf, Philippines	R	*R. mucronata*	6—50	E+	—	E+	—	—	Salmo et al. (2013)
Melbourne, Australia	R	*A. marina*	13—35	E+	—	E+	L+	—	Carnell et al. (2022)
Thai Binh R., Vietnam	R	*K. candel*	3—10		E+	E+	—	—	Cuc et al. (2009)
Central Islands, Philippines	R	*R. apiculata*, *R. mucronata*	15—27	L+	L+	0		L+	Castillo & Breva (2012)
Panay Island, Philippines	R	*R. apiculata*	0.25—30	—	—	E+	E+	—	Ray et al. (2023)
Nakhon Si Thammarat, Thailand	R	*R. apiculata*, *R. mucronata*	10—18	0	0	E+	—	E+	Sakai et al. (2023)
French Guiana coast	NR	*A. germinans*	3—48	—	—	E+	L+	—	Marchand (2017)
French Guiana coast	NR	*A. germinans*, *Rhizophora* spp., *Laguncularia racemosa*	1—>66	E+	E+	L+		E+	Walcker et al. (2018)
Yingluo Bay, China	R, A	*S. apetala*	1—28	Q+[a]	—	L+	—	—	Wang et al. (2021)
Papua, Indonesia	NR	*Rhizophora* spp.	5—25	E+	E+	0	—	L+	Sasmito (2019)
Papua, Indonesia	NR	*R. apiculata*, *Bruguiera* spp.	2—25	L+	L+	0	0	E+	Murdiyarso et al. (2021)
Lamongan, Indonesia	NR	*Rhizophora* spp., *Bruguiera* spp., *A. marina*	15—100	E+	L+	L+	—	L+	Asadi et al. (2017)
N. Sumatra, Indonesia	R	*R. apiculata*, *R. mucronata*	2—30	L+	L+	0		L+	
Jasin, Malaysia	NR	*A. marina*, *Bruguiera cylindrica*, *R. apiculata*	3—25	L+	0	0	0	0	Azman et al. (2023)
Matang, Malaysia	R	*R. apiculata*	1—>70	E+	—	E+	0	E+	Adame et al. (2018)
Sundarbans, Bangladesh	R	*S. apetala*, *A. officinalis*	5—42	E+	E+	0	—	E+	Uddin et al. (2023)
Ayeyarwady delta, Myanmar	R, NR	*Avicennia* spp., *S. apetala*	6—7	E+	E+	0	—	E+	Thant et al. (2012)
Esmeraldas, Ecuador	R, A	*R. mangle*, *A. germinans*, *L. racemosa*	10—21	E+	—	0	—	—	DelVecchia et al. (2014)
Global	R vs. A	Various	1—40	E+	E+	E+	—	E+	Song et al. (2023)
Global	R, A, NR	Various	1—>85	E+	E+	0	0	E+	This study

[a]Total biomass

2012, Abbas et al. 2019, Jones et al. 2019). In at least one Panamanian forest (Jones et al. 2019), aboveground biomass carbon stocks continued to increase beyond 100 yr. Carbon increases in a chronosequence of secondary forests in Costa Rica (Schedlbauer & Kavanagh 2008) was mostly confined to aboveground carbon stocks.

4.2. Lack of global pattern in sediment C_{ORG} stocks versus forest age

In contrast to biomass C_{ORG}–forest age relationships, we found no significant global relationship of sediment C_{ORG} stocks with forest age, at least over the timescale that it takes to accumulate a 1 m sediment deposit. The positive correlations were weak (Figs. 2 & 3), but this is unsurprising given that multiple species and locations encompass many variations in growth patterns across different spatial scales (e.g. intertidal position) and different environmental histories and settings (e.g. carbonate versus deltaic). That is, with increasing stand age, sediment accumulates and C_{ORG} is buried; the annual amount of C_{ORG} input increases with increasing aboveground biomass, at least up to some stable state. As more sediment is deposited, OM gets incorporated into deeper and deeper layers and, thus, is increasingly stabilized. Our results are in contrast with those of Song et al. (2023), who found significant sediment C_{ORG} stock relationships with reforested and afforested stands up to 40 yr old. The differences between both studies may be attributable to the fact that in our analyses there was a wider spread of stand ages (up to 100 yr old) and naturally regenerated stands were included, which resulted in more data points: 333 in this study versus 158 in Song et al. (2023).

There were significant differences in the size of sediment C_{ORG} stocks among plantations of different species (Fig. 3c), with *Bruguiera* spp. and *Kandelia* spp. plantations having greater C_{ORG} stocks than forests dominated by *Avicennia*, *Rhizophora*, and *Sonneratia* species. These results are in contrast with earlier findings (Alongi & Clough 2000, Barreto et al. 2016) of greater sediment C_{ORG} stocks in *Rhizophora* than in *Avicennia* deposits but in agreement with *Kandelia* sediments having higher TOC content and standing stocks than *Sonneratia* sediments (Wu et al. 2020). These differences among genera likely reflect sediment differences in organic chemical composition, the geochemical matrix, position in the intertidal, mode of organic particle capture among species, degree of preservation, pathways of bacterial OM decomposition, and quality and sources of OM (Alongi & Clough 2000, Atwood et al. 2017, Zimmer & Helfer 2021).

An alternative explanation is that the bulk of mangrove sediment, especially beneath the dense live root layer, can be dated to at least the early Holocene, long before the existence of contemporary mangrove forests, leading to asynchronous timescales and lack of a relationship between sediment C_{ORG} stocks and forests of increasing age. Radiocarbon dating (Cohen et al. 2012, Punwong et al. 2013, Andreetta et al. 2014) indicates that subsurface (≥50 cm) mangrove deposits date from 1000 to 4000 ^{14}C cal BP, with sediments increasing in age with greater depth (e.g. >6800 ^{14}C cal BP at 3 m depth; Punwong et al. 2013). Depending on species, climate, and a range of other factors, mangrove trees range in age from 25 to 28 yr for *S. apetala* in the Sundarbans (Rahman et al. 2020) to 48–89 yr for *A. marina* in the arid tropics (Santani et al. 2013) to 80–90 yr for *R. mucronata* in the wet tropics (Verheyden et al. 2004) to 80–100 yr for *R. mangle* in Brazil (Menezes et al. 2003). Thus, mangrove trees exist in a greatly shorter timeframe than the sediments they inhabit. Further, the C_{ORG} in mangrove deposits varies in age with sediment depth and likely includes previous vegetation. For example, the age of humic acid ranged from 11 to 15 yr over the 0–50 cm depth horizon and increased to 459 yr at the 75–100 cm depth interval in subtropical Japanese forests (Kida et al. 2019). In Brazilian mangrove sediments (Behling et al. 2001, Dittmar & Lara 2001, Koch et al. 2005), the estimated age of C_{ORG} ranged from 480 to 680 yr. In restored mangroves in China (Zhang et al. 2012), the age of SOC ranged from 391 to 2512 yr, with the age increasing from the sediment surface to 1 m depth. The asynchrony of tree age and sediment age results in a lack of correlation between these mangrove stand properties, and indicates long-term stability of subsurface C_{ORG} stocks in mangrove sediments.

An additional consideration is that sources of C_{ORG} in mangrove sediments vary in quality and change with stand age, especially in re-established forests (Chen et al. 2018). This applies also to the ratio of autochthonous-to-allochthonous matter, likely reflecting more efficient sediment and particle trapping in older stands (Kathiresan et al. 2013, Soper et al. 2019, Kathiresan et al. 2021, Zimmer & Helfer 2021), and the within-stand source of litter due to changes in species composition upon succession (Quadros et al. 2019). Sediment C_{ORG} stocks depend on the sedimentary history of a given location, and, as for biomass, they are driven by the functional distinctiveness of the local species composition rather than by species richness or functional diversity (Rahman et al. 2021).

There is no global pattern, but several studies have measured increases in sediment C_{ORG} density and content with increasing age of individual stands (Chen et al. 2018, Wiarta et al. 2019, Kathiresan et al. 2021, Wang et al. 2021, Ray et al. 2023, but see Suprayogi et al. 2022 and Zhang et al. 2022 for contrasting results), highlighting large local and regional differences in age-related sediment C_{ORG} stock patterns. C_{ORG} burial and storage rates do not monotonically increase continuously with stand age but level off upon stand maturation (Carnell et al. 2022). Greater total C_{ORG} stocks are often measured in re-established mangrove ecosystems than in pristine forests, and these results may be due to several reasons: (1) higher nutrient levels in restored sediments where 'new' deposits or fertilizers have been added or replanting in abandoned ponds containing nutrient-rich sediments (Chen et al. 2018); (2) rapid growth of comparatively young stands (Kairo et al. 2008); (3) maximization of growth and survival by maximizing planting distance and sound management (Murdiyarso et al. 2022); and (4) enhanced productivity and tree growth through the restoration of tidal connectivity and hydrology (Cormier et al. 2022).

Upon destruction or degradation of mangrove forests, SOM is oxygenated and decayed, resulting in CO_2 release into the atmosphere (Lovelock et al. 2011). In deeper sediment layers that remain protected from disturbance and aeration (Elwin et al. 2019), sediment C_{ORG} stocks may continue to be stable, but this stability will partly depend on the chemical composition, i.e. stability and recalcitrance of the SOM (Zimmer & Helfer 2021). Such a loss of C_{ORG} stocks can be reverted upon natural mangrove recovery or assisted re-establishment. However, even though re-growing or re-planted mangroves restore C_{ORG} stocks over time, the C_{ORG} stocks in the surface sediment of newly established mangrove stands will be comparable to that of conserved mangrove forests only after 20–25 yr (Elwin et al. 2019), and full C_{ORG} stock may take decades or even centuries to recover (Sasmito et al. 2020).

The lack of a significant global relationship between sediment C_{ORG} standing stocks and mangrove forest age mirrors the absence of a clear global pattern in tropical successional and plantation forest soils (Marín-Spiotta & Sharma 2013). A combination of factors was found to drive terrestrial soil C_{ORG} stocks, with the most important variable being mean annual temperature, followed by former land use, soil type, and mean annual precipitation; forest age explained only 10–15% of the total variation, with the strongest age–soil C_{ORG} relationship for sites with no intermediate land use after initial clearing (Marín-Spiotta & Sharma 2013). In naturally regenerated forests in West Kalimantan, Indonesia, severe land use reduced soil C_{ORG} in the topsoil, but C_{ORG} stocks remained unaffected down to 3 m (Borchard et al. 2019). These observations challenge the inclusion of stand age in global estimates of sediment C_{ORG}, and argue for identifying regional factors, e.g. climatic conditions and tidal regimes, to be incorporated into future models for more accurate predictions. In our meta-analysis, mangrove sediment C_{ORG} stocks similarly related best to average annual temperature and precipitation.

4.3. C_{ORG} burial rates

SCBR in re-established mangrove forests were 20% higher than in natural mangrove stands, and although not significantly different, the slightly greater rates may reflect the fact that mangroves are planted in prime restoration or afforestation sites that have been gauged most suitable for maximum growth; proper site selection is a prerequisite for successful restoration (Alongi 2018, Zimmer et al. 2022). Indeed, if all SCBR measured in natural forests are considered in the comparison (169 ± 205 g C m^{-2} yr^{-1}), SCBR in re-established forests are significantly greater, possibly due to greater inputs of allochthonous C_{ORG} and nutrients (Hu et al. 2024). Mangrove SCBR are significantly lower in carbonate settings than in terrigenous settings (Breithaupt & Steinmuller 2022), and, other than a relative handful of plantations in arid, carbonate deposits, most re-establishment activities have been conducted in terrigenous delta, riverine, estuarine, and lagoonal environments (Alongi 2018). This is the rationale for excluding the burial data from carbonate settings from the comparison.

The lack of a SCBR–forest age relationship points to other drivers of blue carbon burial in re-established forests, such as salinity (Section 3.4) and the indirect effects of latitude (Section 3.5), likely reflecting climatic drivers, including storms and geomorphology. Biotic factors such as bioturbation must also be considered (MacKenzie et al. 2021). Data from individual locations (Table 2) indicate that most (6 of 9) studies found no pattern in SCBR with forest age. Ultimately, the rate of C_{ORG} burial depends on the rate of C_{ORG} input to the forest floor minus the rate of bacterial decay. Rates of OM input and bacterial decay, in turn, depend on other drivers, such as intertidal position, bacterial community composition, sedimentary history, geomorphology, distance from terrestrial and marine sources, temperature, and precipitation (Alongi 2018, Breithaupt & Steinmuller 2022).

4.4. Global patterns of ecosystem C_{ORG} trajectories

Total mangrove ecosystem C_{ORG} stocks in re-established mangroves increase globally with increasing forest age, like the global patterns for above- and belowground biomass C_{ORG}. This pattern is somewhat surprising, considering that sediment C_{ORG} stocks, which show no age-related patterns, comprise 67 ± 23% (range: 12–100%) of total ecosystem C_{ORG} stocks over a depth profile of 1 m. In undisturbed natural mangroves, the sediment C_{ORG} stock comprises, on average, 77% of the total ecosystem stock (Alongi 2020b). Thus, the lower percentage in re-established forests is apparently sufficient to allow for a global increase in total ecosystem stocks with forest age. In addition, the percentage range is wide, likely reflecting differences in species composition, forest type, and age from very young monocultures to mature plantations. There were significantly lower ecosystem stocks in *Rhizophora* spp. plantations, suggesting that species of this genus grow more slowly than those of the other genera. For instance, net daytime canopy production of *R. apiculata* in Southeast Asia shows log-phase production until about 20 yr but plateaus thereafter (Alongi 2009). Ecosystem C_{ORG} stocks are also influenced by climatic factors, such as temperature and precipitation, as reflected in the correlation analysis.

Nearly all studies of individual plantations observed either linear or exponential positive trajectories of ecosystem C_{ORG} stocks with increasing forest age (Table 2). As for sediment C_{ORG} stocks, regional age trajectories of total ecosystem C_{ORG} stocks apparently are obscured at a global scale, suggesting vastly varying drivers of stock development over time across regions, forest types, and environmental conditions. Extensive analysis of C_{ORG} stocks and burial in degraded, harvested, converted, and restored mangrove stands in Indonesia (Murdiyarso et al. 2022) revealed that conserved and 30 yr old restored mangrove stands in North Sumatra exhibit highly variable but nearly equivalent total ecosystem C_{ORG} stocks (conserved: 262 ± 70 Mg C ha^{-1}; restored: 349 ± 76 Mg C ha^{-1}) that were higher (albeit not significantly) than in degraded stands (193 ± 62 Mg C ha^{-1}). Across all Indonesian mangrove forests, total ecosystem C_{ORG} stocks were greatest in protected mangroves (mean: 1035 Mg C ha^{-1}) with lower stocks in restored (399 Mg C ha^{-1}), degraded (581 Mg C ha^{-1}), and converted and/or harvested mangroves (250 Mg C ha^{-1}). Nearly all C_{ORG} in degraded and converted stands was vested in the sediment.

In mangrove forests that were selectively logged in Papua, Indonesia (Murdiyarso et al. 2021), sediment C_{ORG} pools were not significantly different among post-logged and protected forests, but total biomass C_{ORG} stocks increased from <50 Mg C ha^{-1} 5 yr after logging to over 100 Mg C ha^{-1} 25 yr since harvesting. As in the present meta-analysis, total ecosystem C_{ORG} stocks showed no clear trajectory with increasing recovery time. A possible explanation could be that C_{ORG} storage rates increase with age during the initial stages of establishment but not further upon maturation (Carnell et al. 2022), and such a maturation stage is reached at different ages in different stands.

Differences in mangrove C_{ORG} stocks in re-established and naturally regenerated stands in one location can often result from natural variations in tidal elevation. In the Can Gio mangrove forests in the Mekong delta, most of the area was replanted 40 yr ago with *R. apiculata* following the end of the Vietnam War (Vinh et al. 2022). Natural regeneration resulted in zonation with (1) a fringe forest dominated by *Avicennia alba*, (2) a transitional forest composed of *R. apiculata*, *A. alba*, *A. officinalis*, and sparse *Excoecaria agallocha* and *Sonneratia alba*, and (3) an inner forest composed of mature *R. apiculata*. Ecosystem C_{ORG} stocks were 150 ± 20, 182 ± 25, 312 ± 28, and 479 ± 33 Mg C ha^{-1} for the adjacent mudflat, fringe, transitional forest, and inner forest, respectively. Zonation differences in C_{ORG} stocks were attributed mostly to sediment characteristics (e.g. redox potential), differences in frequency of tidal inundation, and species-specific differences in productivity and C_{ORG} burial rates (Vinh et al. 2022).

5. CONCLUSIONS

Sediment burial rates of C_{ORG} in re-established versus natural forests are nearly identical, indicating that the re-establishment of mangrove forests is highly viable and a predictable contribution to the additionality of CO_2 removal through nature-based solutions that is needed to meet negative and net-zero emissions that underlie the 1.5° and 2.0°C target of the Paris Agreement. Accurate global estimates of blue carbon stocks in natural (conserved) and re-established mangrove forests would allow for predictive models to reliably forecast mangrove carbon sequestration in both above- and belowground biomass and the sediment, complementing or even replacing time-consuming and challenging measurements under adverse field conditions. The lack of significant relationships between SCBR and increasing forest age indicate that this component of blue carbon may not be essential in formulating predictive

models; the focus therefore should be on age-related changes in forest biomass carbon. Such forecasting would assist in the sustainable development of mangrove plantations and mitigate climate change, possibly through market-based approaches such as PES or carbon finance marketing schemes. However, while stand age was a significant, if highly variable, predictor of biomass C_{ORG} stocks, sediment C_{ORG} stocks, making up the vast majority of total mangrove ecosystem C_{ORG} stocks, were not related to stand age on a global scale. Other drivers of C_{ORG} stocks and dynamics, such as the locally dominant mangrove species and local and regional environmental variables, will have to be incorporated in any attempt to estimate blue carbon sequestration and storage rates and stocks.

Acknowledgements. We thank many of our colleagues, too many to list, for sharing their raw data and additional information with us. We thank Professor Guangcheng Chen, Third Institute of Oceanography, Xiamen, China, for helping to retrieve original Chinese references and helping to translate key elements. M.Z.'s contribution is part of the interdisciplinary research project 'Sea4society—searching for solutions for carbon-sequestration in coastal ecosystems', funded by the Federal Ministry of Education and Research of Germany (BMBF) (project number 03V01653), one of the 6 research consortia of the German Marine Research Alliance (DAM) research mission 'Marine carbon sinks in decarbonization pathways' (CDRmare).

LITERATURE CITED

Abbas S, Nichol JE, Zhang J, Fischer GA (2019) The accumulation of species and recovery of species composition along a 70-year succession in a tropical secondary forest. Ecol Indic 106:105524

Adame MF, Cherian S, Reef R, Stewart-Koster B (2017) Mangrove root biomass and the uncertainty of belowground carbon estimations. For Ecol Manage 403:52–60

Adame MF, Zakaria RM, Fry B, Chong VC, Then YHA, Brown CJ, Lee SY (2018) Loss and recovery of carbon and nitrogen after mangrove clearing. Ocean Coast Manage 161:117–126

Alongi DM (2009) The energetics of mangrove forests. Springer, Dordrecht

Alongi DM (2014) Carbon cycling and storage in mangrove forests. Annu Rev Mar Sci 6:195–219

Alongi DM (2018) Blue carbon: coastal sequestration for climate change mitigation. Springer, Cham

Alongi DM (2020a) Carbon cycling in the world's mangrove ecosystems revisited: significance of non-steady state diagenesis and subsurface linkages between the forest floor and the coastal ocean. Forests 11:977

Alongi DM (2020b) Carbon balance in salt marsh and mangrove ecosystems: a global synthesis. J Mar Sci Eng 8:767

Alongi DM (2022) Impacts of climate change on blue carbon stocks and fluxes in mangrove forests. Forests 13:149

Alongi DM, Clough BF (2000) Below-ground decomposition of organic matter in forests of the mangroves *Rhizophora stylosa* and *Avicennia marina* along the arid coast of Western Australia. Aquat Bot 68:97–122

Andreetta A, Fusi M, Cameldi I, Cimó F, Carnicelli S, Cannicci S(2014) Mangrove carbon sink. Do burrowing crabs contribute to sediment carbon storage? Evidence from a Kenyan mangrove system. J Sea Res 85:524–533

Asadi MA, Guntur G, Ricky AB, Novianti P, Andik I (2017) Mangrove ecosystem C-stocks of Lamongan, Indonesia and its correlation with forest age. Res J Chem Environ 21:1–9

Atwood TB, Connolly RM, Almahasheer H, Carnell PE and others (2017) Global patterns in mangrove soil carbon stocks and losses. Nat Clim Chang 7:523–528

Azman MS, Sharma S, Hamzah ML, Zakaria RM, Palaniveloo K, MacKenzie RA (2023) Total ecosystem blue carbon stocks and sequestration potential along a naturally regenerated mangrove forest chronosequence. For Ecol Manage 527:120611

Barreto MB, Lo Mónaco S, Díaz R, Barreto-Pittol E, López L, Peralba MDCR (2016) Soil organic carbon of mangrove forests (*Rhizophora* and *Avicennia*) of the Venezuelan Caribbean coast. Org Geochem 100:51–61

Behling H, Cohen MCL, Lara RJ (2001) Studies on Holocene mangrove ecosystem dynamics of the Bragança Peninsula in north-eastern Pará, Brazil. Palaeogeogr Palaeoclimatol Palaeoecol 167:225–242

Borchard N, Bulusu M, Meyer N, Rodionov A and others (2019) Deep soil storage in tree-dominated land use systems in tropical lowlands of Kalimantan. Geoderma 354: 113864

Breithaupt JL, Steinmuller HE (2022) Refining the global estimate of mangrove carbon burial rates using sedimentary and geomorphic setting. Geophys Res Lett 49: e2022GL100177

Breithaupt JL, Smoak JM, Smith TJ III, Sanders CJ, Hoare A (2012) Organic carbon burial rates in mangrove sediments: strengthening the global budget. Global Biogeochem Cycles 26:GB3011

Breithaupt JL, Steinmuller HE, Rovai AS, Engelbert KM and others (2023) An improved framework for estimating organic carbon content of mangrove soils using loss-on-ignition and coastal environmental settings. Wetlands 43: 57

Carnell PE, Palacios MM, Waryszak P, Trevathan-Tackett SM, Masqué P, Macreadie PI (2022) Blue carbon drawdown by restored mangrove forests improves with age. J Environ Manage 306:114301

Castillo JAA, Breva LA (2012) Carbon stock assessment for four mangrove reforestation/plantation stands in the Philippines. In: Palis HG, Pasicolam SA, Villamor CI (eds) Proc 1st ASEAN Congress on Mangrove Research and Development, 3–7 December 2012, Manila. Department of Environment and Natural Resources, Manila, p 244–254

Chen G, Gao M, Pang B, Chen S, Ye Y (2018) Top-meter sediment organic carbon stocks and sources in restored mangrove forests of different ages. For Ecol Manage 422: 87–94

Chen J, Zhai G, Chen G, Wu J and others (2023) Differences in ecosystem organic carbon stocks due to species selection and site elevation of restored mangrove forests. Catena 226:107089

Cohen MCL, Pessenda LCR, Behling H, Rossetti DF and others (2012) Holocene paleoenvironmental history of the Amazonian mangrove belt. Quat Sci Rev 55:50–58

Cormier N, Krauss KW, Demopoulos AWJ, Jessen BJ, McClain-Counts JP (2022) Potential for carbon and nitrogen sequestration by restoring tidal connectivity and enhancing sediment surface elevations in denuded and degraded South Florida mangrove ecosystems. In: Krauss KW, Zhu Z, Stagg CL (eds) Wetland carbon and environmental management. Wiley, Hoboken, NJ, p 143–158

Cuc NTK, Ninomiya I, Long NT, Tri NH, Tuan MS (2009) Belowground carbon accumulation in young *Kandelia candel* (L.) Blanco plantations in Thai Binh River mouth, Northern Vietnam. Int J Econ Dev 12:107–117

DelVecchia AG, Bruno JF, Benninger L, Alperin M, Banerjee O (2014) Organic carbon inventories in natural and restored Ecuadorian mangrove forests. PeerJ 2:e388

Dittmar T, Lara RJ (2001) Molecular evidence for lignin degradation in sulfate-reducing mangrove sediment (Amazônia, Brazil). Geochim Cosmochim Acta 65: 1417–1428

Elwin A, Bukoski JJ, Jintana V, Robinson EJ, Clark JM (2019) Preservation and recovery of mangrove ecosystem carbon stocks in abandoned shrimp ponds. Sci Rep 9: 18275

Fourqurean J, Johnson B, Kauffman JB, Kennedy H, Lovelock C, Alongi DM (2015) Field sampling of soil carbon pools in coastal ecosystems. In: Howard J, Hoyt S, Isensee K, Telszewski M, Pigeon E (eds) Blue carbon: methods for assessing carbon stocks and emissions factors in mangroves, tidal salt marshes, and seagrasses. Conservation International, Intergovernmental Oceanic Commission, UNESCO, IUCN, Arlington, VA, p 41–66

Friess DA, Adams J, Andradi-Brown DA, Bhargava R and others (2024) Mangrove forests: their status, threats, conservation and restoration. In: Baird D, Elliott ME (eds) Treatise on estuarine and coastal science, 2nd edn. Academic Press, New York, NY, p 1–29

Gevaña DT, Camacho LD, Camacho SC (2017) Stand density management and blue carbon stock of monospecific mangrove plantation in Bohol, Philippines. For Stud 66: 75–83

Goldberg L, Lagomasino D, Thomas N, Fatoyinbo T (2020) Global declines in human-driven mangrove loss. Glob Change Biol 26:5844–5855

He Z, Sun H, Peng Y, Hu Z, Cao Y, Lee SY (2020) Colonization by native species enhances the carbon storage capacity of exotic mangrove monocultures. Carbon Balance Manag 15:28

Hien HT, Marchand C, Aime J, Cuc NTK (2018) Seasonal variability of CO_2 emissions from sediments in planted mangroves. (Northern Viet Nam). Estuar Coast Shelf Sci 213:28–39

Hieu PV, Dung LV, Tu NT, Omori K (2017) Will restored mangrove forests enhance sediment organic carbon and ecosystem carbon storage? Reg Stud Mar Sci 14:43–52

Hilmi N, Chami R, Sutherland MD, Hall-Spencer JM, Lebleu L, Benitez MB, Levin LA (2021) The role of blue carbon in climate change mitigation and carbon stock conservation. Front Clim 3:710546

Howard J, Hoyt S, Isensee K, Telszewski M, Pidgeon E (eds) (2014) Coastal blue carbon: methods for assessing carbon stocks and emissions factors in mangroves, tidal salt marshes, and seagrasses. IUCN, Arlington, VA

Hu J, Pradit S, Loh PS, Chen Z and others (2024) Storage and dynamics of soil organic carbon in allochthonous-dominated and nitrogen-limited natural and planted mangrove forests in southern Thailand. Mar Pollut Bull 200: 116064

Jones IL, DeWalt SJ, Lopez OR, Bunnefeld L, Pattison Z, Dent DH (2019) Above- and belowground carbon stocks are decoupled in secondary tropical forests and are positively related to forest age and soil nutrients respectively. Sci Total Environ 697:133987

Kairo JG, Lang'at JKS, Dahdouh-Guebas F, Bosire J, Karachi M (2008) Structural development and productivity of replanted mangrove plantations in Kenya. For Ecol Manage 255:2670–2677

Kathiresan K, Anburaj R, Gomathi V, Saravanakumar K (2013) Carbon sequestration potential of *Rhizophora mucronata* and *Avicennia marina* as influenced by age, season, growth, and sediment characteristics in southeast coast of India. J Coast Conserv 17:397–408

Kathiresan K, Rajendran N, Balakrishnan B, Thiruganasambandam R, Narayanasamy R (2021) Carbon sequestration and storage in planted mangrove stands of *Avicennia marina*. Reg Stud Mar Sci 43:101701

Kida M, Kondo M, Tomotsune M, Kinjo K, Ohtsuka T, Fujitake N (2019) Molecular composition and decomposition stages of organic matter in a mangrove mineral soil with time. Estuar Coast Shelf Sci 231:106478

Koch BP, Harder J, Lara RJ, Kattner G (2005) The effect of selective microbial degradation on the composition of mangrove derived pentacyclic triterpenols in surface sediments. Org Geochem 36:273–285

Komiyama A, Ong JE, Poungparn S (2008) Allometry, biomass, and productivity of mangrove forests: a review. Aquat Bot 89:128–137

Lovelock CE, Ruess RW, Feller IC (2011) CO_2 efflux from cleared mangrove peat. PLOS ONE 6:e21279

Lovelock CE, Adame MF, Butler DW, Kelleway JJ and others (2022) Modeled approaches to estimating blue carbon accumulation with mangrove restoration to support a blue carbon accounting method for Australia. Limnol Oceanogr 67:S50–S60

MacKenzie R, Sharma S, Rovai AR (2021) Environmental drivers of blue carbon burial and sediment carbon stocks in mangrove forests. In: Sidik F, Friess DA (eds) Dynamic sedimentary environments of mangrove coasts. Elsevier, Amsterdam, p 275–294

Marchand C (2017) Soil carbon stocks and burial rates along a mangrove forest chronosequence (French Guiana). For Ecol Manage 384:92–99

Marín-Spiotta E, Sharma S (2013) Carbon storage in successional and plantation forest soils: a tropical analysis. Glob Ecol Biogeogr 22:105–117

Menezes M, Berger U, Worbes M (2003) Annual growth rings and long-term growth patterns of mangrove trees from the Bragança peninsula, North Brazil. Wetlands Ecol Manage 11:233–242

Murdiyarso D, Sasmito SD, Sillanpää M, MacKenzie R, Gaveau D (2021) Mangrove selective logging sustains biomass carbon recovery, sediment carbon, and sediment. Sci Rep 11:12325

Murdiyarso D, Arifanti VB, Sidik F, Sillanpää M, Sasmito SD (2022) Optimizing carbon stocks and sedimentation in Indonesian mangroves under different management regimes. In: Krauss KW, Zhu Z, Stagg CL (eds) Wetland carbon and environmental management. Wiley, Hoboken, NJ, p 159–172

Page MJ, McKenzie JE, Bossuyt PM, Boutron I and others (2021) The PRISMA 2020 statement: an updated guide-

line for reporting systematic reviews. Int J Surg 88: 105906
Punwong P, Marchant R, Selby K (2013) Holocene mangrove dynamics in Makoba Bay, Zanzibar. Palaeogeogr Palaeoclimatol Palaeoecol 379–380:54–67
Quadros AF, Nordhaus I, Reuter H, Zimmer M (2019) Modelling of mangrove annual leaf litterfall with emphasis on the role of vegetation structure. Estuar Coast Shelf Sci 218:292–299
Rahman MM, Zimmer M, Ahmed I, Donato D, Kanzaki M, Xu M (2021) Co-benefits of protecting mangroves for biodiversity conservation and carbon storage. Nat Commun 12:3875
Rahman MS, Sass-Klaassen U, Zuidema PA, Chowdhury Md Q, Beeckman H (2020) Salinity drives growth dynamics of the mangrove tree *Sonneratia apetala* Buch. - Ham in the Sundarbans, Bangladesh. Dendrochronologia 62: 125711
Ray R, Suwa R, Miyajima T, Munar J and others (2023) Sedimentary blue carbon dynamics based on chronosequential observations in a tropical restored mangrove forest. Biogeosciences 20:911–928
Rosentreter JA, Al-Haj, AN, Fulweiler RW, Williamson P (2021) Methane and nitrous oxide emissions complicate coastal blue carbon assessments. Global Biogeochem Cycles 35:e2020GB006858
Rosentreter JA, Laruelle GG, Bange HW, Bianchi TS and others (2023) Coastal vegetation and estuaries are collectively a greenhouse gas sink. Nat Clim Chang 13:579–587
Sakai Y, Kouyama T, Kakinuma K, Sakaguchi Y and others (2023) Recovery of mangrove ecosystem carbon through reforestation at abandoned shrimp ponds in Southeast Thailand. Ecosyst Health Sustain 9:0018
Salmo SG III, Lovelock CE, Duke NC (2013) Vegetation and sediment characteristics as indicators of restoration trajectories in restored mangroves. Hydrobiologia 720:1–18
Santini NS, Hua Q, Schmitz N, Lovelock CE (2013) Radiocarbon dating and wood density chronologies of mangrove trees in arid Western Australia. PLOS ONE 8:e80116
Sasmito SD (2019) Mangrove blue carbon dynamics in Papua, Indonesia: effects of hydro-geomorphic setting and land-use. PhD dissertation, Charles Darwin University, Darwin
Sasmito SD, Kuzyakov Y, Lubis AA, Murdiyarso D and others (2020) Organic carbon burial and sources in sediments of coastal mudflat and mangrove ecosystems. Catena 187: 104414
Schedlbauer JL, Kavanagh KL (2008) Soil carbon dynamics in a chronosequence of secondary forests in northeastern Costa Rica. For Ecol Manage 255:1326–1335
Sierra CA, del Valle JI, Restrepo HI (2012) Total carbon accumulation in a tropical forest landscape. Carbon Balance Manag 7:12
Song S, Ding Y, Li W, Men Y and others (2023) Mangrove reforestation provides greater blue carbon benefit than afforestation for mitigating global climate change. Nat Commun 14:756
Soper FM, MacKenzie RA, Sharma S, Cole TG, Litton CM, Sparks JP (2019) Non-native mangroves support carbon storage, sediment carbon burial, and accretion of coastal ecosystems. Glob Change Biol 25:4315–4326
Su J, Friess DA, Gasparatos H (2021) A meta-analysis of the ecological and economic outcomes of mangrove restoration. Nat Commun 12:5050
Suprayogi B, Purbopuspito J, Suriani Harefa M, Panjaitan GY, Nasution Z (2022) Ecosystem carbon stocks of restored mangroves and its sequestration in northern Sumatra coast, Indonesia. Univers J Agric Res 10:1–19
Syms C (2019) Principal components analysis. In: Fath B (ed) Encyclopedia of ecology, 2nd edn, Vol 3. Elsevier, Amsterdam, p 566–573
Thant YM, Kanzaki M, Ohta S, Than MM (2012) Carbon sequestration by mangrove plantations and a natural regeneration stand in the Ayeyarwady Delta, Myanmar. Tropics 21:1–10
Uddin MM, Aziz AA, Lovelock CE (2023) Importance of mangrove plantations for climate change mitigation in Bangladesh. Glob Change Biol 29:3331–3346
Verheyden A, Kairo JG, Beeckman H, Koedam N (2004) Growth rings, growth ring formation and age determination in the mangrove *Rhizophora mucronata.* Ann Bot 94: 59–66
Vinh TV, Marchand C, Linh KT, Jacotot A, Nguyen TH, Allenbach M (2022) Soil and aboveground carbon stocks in a planted tropical mangrove forest (Can Gio, Vietnam). In: Krauss KW, Zhr Z, Stagg CL (eds) Wetland carbon and environmental management. Wiley, Hoboken, NJ, p 229–245
Walcker R, Gandois L, Proisy C, Corenblit D and others (2018) Control of 'blue carbon' storage by mangrove aging: evidence from a 66-year chronosequence in French Guiana. Global Change Biol 24:2325–2338
Wang G, Yu C, Singh M, Guan D, Xiong Y, Zheng R, Xiao R (2021) Community structure and ecosystem carbon stock dynamics along a chronosequence of mangrove plantations in China. Plant Soil 464:605–620
Wiarta R, Indrayani Y, Mulia F, Astiani D (2019) Carbon sequestration by young *Rhizophora apiculata* plants in Kubu Raya District, West Kalimantan, Indonesia. Biodiversitas 20:311–315
Wu M, He Z, Fung S, Cao Y, Guan D, Peng Y, Lee SY (2020) Species choice in mangrove reforestation may influence the quantity and quality of long-term carbon sequestration and storage. Sci Total Environ 714:136742
Yu C, Feng J, Liu K, Wang G, Zhu Y, Chen H, Guan D (2020) Changes in ecosystem carbon stock following the plantation of exotic mangrove *Sonneratia apetala* in Qi'ao Island, China. Sci Total Environ 717:137142
Yu C, Guan D, Gang W, Lou D, Wei L, Zhou Y, Feng J (2021) Development of ecosystem carbon stock with the progression of a natural mangrove forest in Yingluo Bay, China. Plant Soil 460:391–401
Zhang JP, Shen CD, Ren H, Wang J, Han WD (2012) Estimating change in sedimentary organic carbon content during mangrove restoration in Southern China using carbon isotopic measurements. Pedosphere 22:58–66
Zhang Z, Wang Y, Zhu Y, He K and others (2022) Carbon sequestration in soil and biomass under native and non-native mangrove ecosystems. Plant Soil 479:61–76
Zimmer M, Helfer V (2021) Quantity and quality of organic matter in mangrove sediments. In: Sidik F, Friess DA (eds) Dynamic sedimentary environments of mangrove coasts. Elsevier, Amsterdam, p 369–391
Zimmer M, Ajonina GN, Amir AA, Cragg S and others (2022) When nature needs a helping hand: different levels of human intervention for mangrove (re-)establishment. Front For Glob Change 5:784322

Appendix.

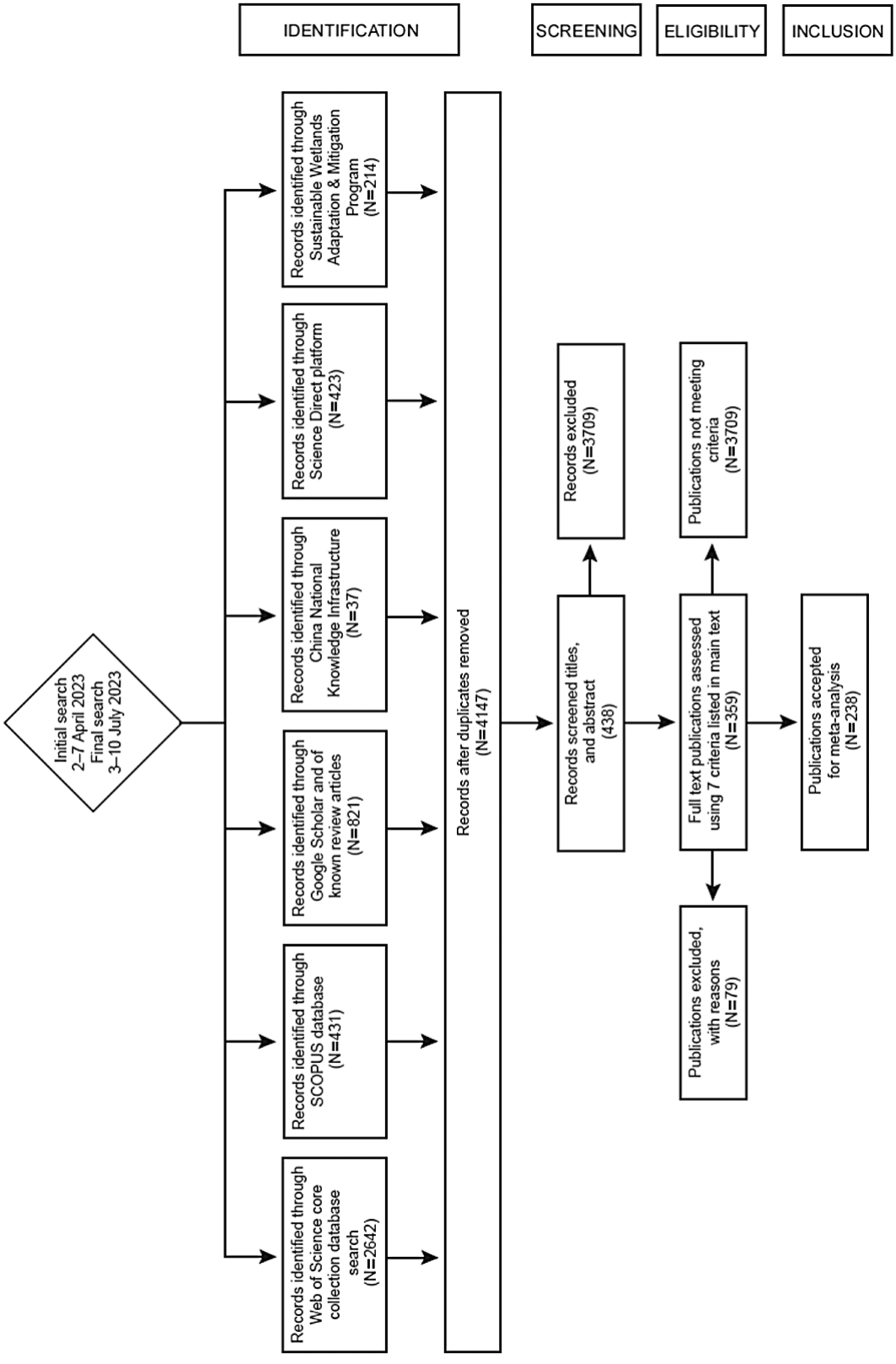

Fig. A1. Schematic of the PRISMA protocol followed in the initial and final searches for publications in performing the meta-analysis. See Section 2.1 for further details

Editorial responsibility: Erik Kristensen, Odense, Denmark
Reviewed by: 3 anonymous referees

Submitted: November 27, 2023
Accepted: February 12, 2024
Proofs received from author(s): March 30, 2024